CROSS-CORRELATION FUNCTIONS FOR A NEURONAL MODEL

C. K. KNOX

From the Laboratory of Neurophysiology, Department of Physiology, University of Minnesota, Minneapolis, Minnesota 55455

ABSTRACT Cross-correlation functions, $R_{XY}(t,\tau)$, are obtained for a neuron model which is characterized by constant threshold θ, by resetting to resting level after an output, and by membrane potential $U(t)$ which results from linear summation of excitatory postsynaptic potentials $h(t)$. The results show that: (*1*) Near time lag $\tau = 0, R_{XY}(t,\tau) = f_U[\theta - h(\tau), t + \tau]\{h'(\tau) + E_U[u'(t + \tau)]\}$ for positive values of this quantity, where $f_U(u,t)$ is the probability density function of $U(t)$ and $E_U[u'(t + \tau)]$ is the mean value function of $U'(t + \tau)$. (*2*) Minima may appear in $R_{XY}(t,\tau)$ for a neuron subjected only to excitation. (*3*) For large τ, $R_{XY}(t,\tau)$ is given approximately by the convolution of the input autocorrelation function with the functional of point (*1*). (*4*) $R_{XY}(t,\tau)$ is a biased estimator of the shape of $h(t)$, generally overestimating both its time to peak and its rise time.

INTRODUCTION

The inability to record intracellularly from many neurons of the central nervous system makes the use of cross-correlation techniques particularly intriguing for assessing internal parameters of a neural system based on extracellularly recorded spike activity. Although these techniques have been used experimentally their theoretical bases on which interpretations of data can be made are poorly understood. Previous work has shown that the cross-correlation function evidences two types of neural effects: *primary synaptic* and *secondary or periodicity effects* (Moore et al., 1970). Periodicity effects arise from pacemaker activity within the cells of the system, and it has been suggested that primary synaptic effects result from a linear transformation of the postsynaptic potential (PSP) (Moore et al., 1970). In a more recent study, however, Bryant et al. (1973) found no simple linear correspondence between primary synaptic effect and PSP. This is not surprising in view of the nonlinear nature of the nerve cell. In fact, intuitively one does not expect a correlation over the entire time course of the PSP since it is only during the rising phase of the membrane potential that the possibility exists of crossing the threshold for nerve impulse generation. If the average drift of membrane potential towards threshold is low or absent altogether, then correlation will exist largely during the rising phase of the PSP.

To provide some theoretical understanding of the cross-correlation function at the unit level I have analyzed the problem of primary synaptic effect in detail using a

simplified model of the neuron which incorporates the principal features of the cell. The model is characterized by constant threshold, by resetting to resting level and by excitatory PSPs such as the unit step function $w(t)$, the exponential exp $(-\epsilon t)$ and more general shapes. Numerical solutions are obtained when the model is driven by random synaptic input with no inherent pacemaker activity or internal noise.

MATHEMATICAL DERIVATIONS

Statement of the Model

The model I consider (Fig. 1) is a somewhat generalized version of one used by previous investigators (Fetz and Gerstein, 1963; Stein, 1965). Spikes arrive at random over a single excitatory channel and are here idealized as Dirac delta functions, $X(t) = \sum_k \delta(t - t_k)$. $X(t)$ is assumed to be a stationary renewal process and the density function for the times between spikes in $X(t)$ will be denoted $f_X(x)$. Following a resetting to zero at time t_0, the *membrane potential*

$$U(t) = \int_{t_0}^{t} X(\tau)\, h(t - \tau)\, d\tau,$$

or

$$U(t) = \sum_k h(t - t_k), t_0 \leq t_k,$$

so long as $U(t)$ remains less than constant threshold θ. The implicit assumption of linear summation of $h(t)$ is considered reasonable in the subthreshold region. Upon reaching threshold an output pulse is generated and $U(t)$ is reset to zero where summation begins anew with no refractory period. Between each pair of spikes in the output process $Y(t)$, the membrane potential may be viewed in general as one realization of a developing shot process (Rice, 1944; Parzen, 1962). The probability density function for the membrane potential will be denoted $f_U(u, t - t_j), t \geq t_j$, where t_j are the times of occurrence of output spikes, or more simply $f_U(u, t)$. For $h(t)$'s which decay with time and large $t - t_j$, $f_U(u, t - t_j) = f_U(u, t) \rightarrow f_U(u)$, independent of time.

The distribution of times between spikes in $Y(t)$ is unknown in general. Johannesma

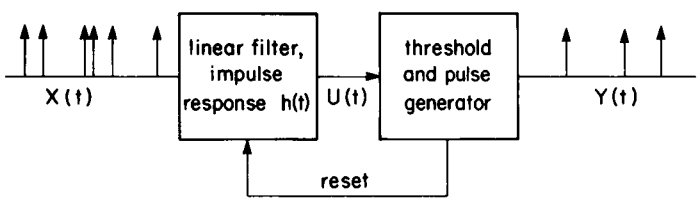

FIGURE 1 Neuron model. The input pulse train $X(t)$ is filtered to produce the potential $U(t)$. When $U(t)$ reaches a constant threshold an output pulse is generated and $U(t)$ is reset to zero.

(1968) has obtained a linear inhomogeneous partial differential-difference equation for $f_U(u,t)$ when $h(t)$ is of the form $\exp(-\epsilon t)$ and $X(t)$ is Poisson. However, there are no known solutions to the equation subject to the boundary conditions $f_U(u,0) = \delta(u)$ and $f_U(\theta,t) = 0$. When $h(t) \ll \theta$ he is able to produce the moments of the first passage time distribution. Obviously, when $h(t)$ is the unit step function and n is the next integer $\geq \theta \geq 1$, times between spikes in $Y(t)$ are distributed according to the sum of n intervals of $X(t)$.

The Perfect Integrator

While this is a relatively simple case of the model, it is included here to introduce nomenclature and to illustrate the method I use to derive the cross-correlation function for more complicated $h(t)$'s. The conclusions of this section, namely that the perfect integrator neuron is a simple rate divider attenuating all frequency components at the input a constant amount have been reached differently by other investigators (Stein et al., 1972; Knight, 1972).

The cross-correlation function is given by the expected value of the product of $Y(t+\tau)$ and $X(t)$, where the lag τ is taken here to be positive.

$$R_{XY}(t,\tau) = E[Y(t+\tau)X(t)],$$

or in terms of conditional expectation

$$R_{XY}(t,\tau) = E[Y(t+\tau) \mid X(t)]E[X(t)]. \tag{1}$$

Since the system is causal, $R_{XY}(t,\tau)$ is simply the product of the input and output rates when τ is negative. If the probability of occurrence of a spike in $X(t)$ in t, $t+\Delta t$ is $\lambda\Delta t$ then $E[X(t)] = \lim_{\Delta t \to 0}(1/\Delta t)\cdot\lambda\Delta t = \lambda$, the mean rate. Therefore,

$$R_{XY}(t,\tau) = \lambda E[Y(t+\tau) \mid X(t)]. \tag{2}$$

Similarly, $Y(t)$ is approximately either $1/\Delta t$ or 0 and if $r_{Y|X}(t,\tau)\Delta t$ denotes the probability of an event in Y in $t+\tau$, $t+\tau+\Delta t$ given an event in X in t, $t+\Delta t$, then

$$R_{XY}(t,\tau) = \lambda r_{Y|X}(t,\tau). \tag{3}$$

Now, $r_{Y|X}(t,\tau)$ is the probability density for the occurrence of a spike in Y given *any* preceding spike in X. This spike in X could be the one immediately preceding an output spike, the second preceding, etc. Denoting these possibilities with subscript $Y|1$, $Y|2$, etc., in general

$$R_{XY}(t,\tau) = \lambda \sum_{k=1}^{\infty} r_{Y|k}(t,\tau). \tag{4}$$

Consider $r_{Y|1}$. Given the first preceding input spike, unless $\tau = 0$, the probability of

observing an output is zero. If at $\tau = 0$ $U(t)$ falls between $n - 1$ and n (where n was defined previously as the next integer $\geq \theta \geq 1$) then an output will occur. That is,

$$r_{Y|1} = P[n - 1 < U(t) \leq n]\,\delta(\tau),$$

where P denotes probability. Now, for the perfect integrator $P[n - 1 < U(t) \leq n] = P[n-2 < U(t) \leq n - 1] \ldots = 1/n$. Therefore,

$$r_{Y|1} = \delta(\tau)/n.$$

Consider $r_{Y|2}$. Given the second preceding input spike, an output will occur at time $t + \tau$ if the interval between the two preceding input spikes is τ *and* at time t $U(t)$ falls between $n - 2$ and $n - 1$, so that

$$r_{Y|2} = f_X(\tau)/n.$$

For $r_{Y|3}$, two intervals in $X(t)$ must sum to τ, hence

$$r_{Y|3} = f_X(\tau) * f_X(\tau)/n,$$

where the asterisk denotes convolution.

By induction, Eq. 4 thus becomes

$$R_{XY}(\tau) = (\lambda/n)[\delta(\tau) + f_X(\tau) + f_X(\tau) * f_X(\tau) + f_X(\tau) * f_X(\tau) * f_X(\tau) + \ldots]. \quad (5)$$

λ times the quantity in square brackets is the autocorrelation function of the input process (Bartlett, 1963). For a linear system the cross-correlation function is given by the convolution of the input autocorrelation function with the impulse response of the system. In a sense then the model behaves as a linear system with a stochastic impulse response of $\delta(t)/n$. It is not linear in the strict sense as there may not be an output for any given input. When outputs occur, however, Eq. 5 implies that they occur precisely at the time of an input spike.

When $X(t)$ is a Poisson process

$$R_{XY}(\tau) = (\lambda/n)[\delta(\tau) + \lambda]. \quad (6)$$

The Leaky Integrator, $h(t) = a \exp(-\epsilon t)$

Proceeding in the same manner as in the previous section

$$r_{Y|1} = \delta(\tau)\,P[\theta - a < U(t) \leq \theta].$$

In this case $f_U(u,t)$ is a function of both u and t but its form is not known in the general case. Later in this paper I approximate $f_U(u,t)$ with $f_U(u)$ for the developed shot process when $X(t)$ is Poisson in which case the characteristic function is known.

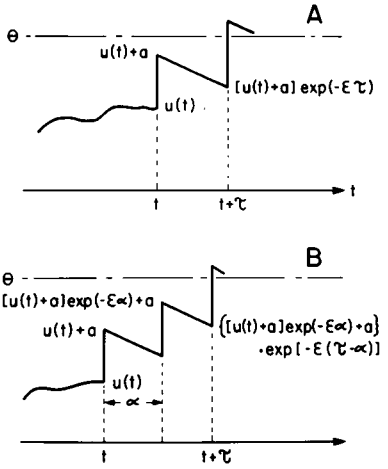

FIGURE 2 Typical potential profile for two (A) and three (B) inputs leading to an output. The filter impulse response is $a \cdot \exp(-\epsilon t)$, the potential is $u(t)$ at time t and attains the values shown at the arrival times of the input pulses. The probability of an output at $t + \tau$ is given by the probability that the potential falls within θ and $\theta - a$ at time $t + \tau$ and that the intervals between inputs place an input pulse at time $t + \tau$.

To derive the next higher order terms of Eq. 4 consider Figs. 2 A and 2 B which apply to the cases of two and three preceding input spikes. An output will occur at time $t + \tau$ on two successive input spikes if the interval between them is τ and the membrane potential at time $t + \tau$ falls between θ and $\theta - a$, i.e.,

$$r_{Y|2} = f_X(\tau)\, P[\theta - a < U(t + \tau) \leq \theta].$$

Since $U(t + \tau) = [U(t) + a] \exp(-\epsilon\tau)$, in this instance,

$$\begin{aligned} r_{Y|2} &= f_X(\tau)\, P[(\theta - a) \exp \epsilon\tau - a < U(t) \leq \theta \exp \epsilon\tau - a], \\ &= f_X(\tau)\, P_2(t, \tau) \geq 0. \end{aligned}$$

In like fashion,

$$r_{Y|3} = \int_0^\tau f_X(\alpha)\, f_X(\tau - \alpha)\, P[\theta - a < U(t + \tau) \leq \theta]\, d\alpha,$$

or

$$r_{Y|3} = \int_0^\tau f_X(\alpha)\, f_X(\tau - \alpha)\, P[(\theta - a) \exp \epsilon\tau - a(1 + \exp \epsilon\alpha) < U(t) \leq \theta \exp \epsilon\tau - a(1 + \exp \epsilon\alpha)]\, d\alpha$$

$$r_{Y|3} = \int_0^\tau f_X(\alpha)\, f_X(\tau - \alpha)\, P_3(t, \tau, \alpha)\, d\alpha.$$

Also,

$$r_{Y|4} = \int_0^{\tau} f_X(\alpha) \int_0^{\tau-\alpha} f_X(\beta) f_X(\tau - \alpha - \beta) P[(\theta - a)\exp \epsilon\tau - a\exp \epsilon\alpha$$

$$- a\exp \epsilon(\alpha + \beta) - a < U(t) \leq \theta\exp \epsilon\tau - a\exp \epsilon\alpha - a\exp \epsilon(\alpha + \beta) - a] \mathrm{d}\beta\, \mathrm{d}\alpha$$

or

$$r_{Y|4} = \int_0^{\tau} f_X(\alpha) \int_0^{\tau-\alpha} f_X(\beta) f_X(\tau - \alpha - \beta) P_4(t, \tau, \alpha, \beta) \mathrm{d}\beta\, \mathrm{d}\alpha,$$

etc. The sum of these terms and higher order ones is equal to and defines $R_{XY}(t, \tau)$.

It is possible to make approximations to the $r_{Y|k}$ particularly for higher orders. The $r_{Y|k}$ are convolutions of interval densities with respect to a weight function $P[\cdot]$. The means of the densities $r_{Y|k}$ increase with k. As the means become large with respect to the time over which the membrane potential remains correlated one can allow $P[\theta - a < U(t + \tau) \leq \theta]$ to be approximately $P[\theta - a < U(t) \leq \theta]$. For large k, then

$$r_{Y|k} \cong P[\theta - a < U(t) \leq \theta] f_X(\tau)^{*(k-2)}, k \gg 1 \tag{7}$$

where $f_X(\tau)^{*(k-2)}$ denotes the $k - 2$ convolution of $f_X(\tau)$ with itself. In all cases, by the same reasoning, as τ becomes large

$$R_{XY}(t, \tau) \cong \lambda P[\theta - a < U(t) \leq \theta]$$
$$\cdot [f_X(\tau) + f_X(\tau) * f_X(\tau) + f_X(\tau) * f_X(\tau) * f_X(\tau) + \cdots], \tag{8}$$

or proportional to the autocorrelation function of the input. Just as in the case of the ideal integrator the proportionality factor is the probability that the membrane potential falls within one shot of threshold. Here, however, this factor is not constant but depends among other things on the mean rate of events in the input process $X(t)$.

When $X(t)$ is a Poisson process $f_X(\tau) = \lambda \exp(-\lambda\tau)$ and it follows that

$$R_{XY}(t, \tau) \cong \lambda[\delta(\tau) + \lambda - (\lambda + \lambda^2\tau + \lambda^3\tau^2/2)\exp(-\lambda\tau)]$$
$$\cdot P[\theta - a < U(t) \leq \theta]$$
$$+ [\lambda P_2 + \lambda^2 \int_0^{\tau} P_3 d\alpha + \lambda^3 \int_0^{\tau} \int_0^{\tau-\alpha} P_4 \mathrm{d}\beta\, \mathrm{d}\alpha] \exp(-\lambda\tau), \tag{9}$$

where $r_{Y|5}$ and higher have been approximated with Eq. 7 and $f_X(\tau)^{*(k-2)} = \lambda^{k-1} \tau^{k-2}\exp(-\lambda\tau)/(k - 2)!$

More General h(t)'s

It does not seem possible to me to obtain explicit results for the cross-correlation function for more complicated $h(t)$'s other than those considered owing to the fact that

$U(t + \tau)$ can no longer be simply related to $U(t)$. Nevertheless, it is constructive to consider the first few $r_{Y|k}(t, \tau)$ so that at least the general form of the cross-correlation function may be appreciated.

In the previous two cases $h(t)$ rises instantaneously at time 0 to a new value. This produces a delta function in the cross-correlation in term $r_{Y|1}$. For arbitrary $h(t)$, $r_{Y|1}$ is given by the probability that at time $t + \tau$ the membrane potential passes through a $du(t + \tau)$ about $u(t + \tau) = \theta - h(\tau)$ with positive slope, i.e., $du(t + \tau) = [h'(\tau) + u'(t + \tau)]\, dt$ for a particular realization of $U(t)$. Therefore,

$$r_{Y|1}(t, \tau) = f_U[\theta - h(\tau), t + \tau] \cdot [h'(\tau) + u'(t + \tau)],$$

for $h'(\tau) + u'(t + \tau) \geq 0$.

For all possible paths $U(t)$, Eq. 2 may be written in the form

$$R_{XY}(t, \tau) = \lambda E_U\{E[Y(t + \tau) \mid X(t) \text{ and } U(t)]\}$$

or in terms of $r_{Y|k}$

$$R_{XY}(t, \tau) = \lambda \sum_{k=1}^{\infty} E_U[r_{Y|k}(t, \tau)]. \tag{10}$$

Thus,

$$E_U[r_{Y|1}(t, \tau)] = f_U[\theta - h(\tau), t + \tau] \cdot \{h'(\tau) + E_U[u'(t + \tau)]\}.$$

Since this term describes the behavior of $R_{XY}(t, \tau)$ near $\tau = 0$, it can be seen that correlation exists beyond the time to peak of $h(t)$ if membrane potential drifts, on average, towards threshold.

Reasoning as in the previous sections, average values of $r_{Y|2}$ and $r_{Y|3}$ can be shown to be given by

$$E_U[r_{Y|2}(t, \tau)] = \int_0^{\tau} f_X(\tau - \alpha) f_U[\theta - h(\tau) - h(\alpha), t + \tau] \cdot \{h'(\tau) + h'(\alpha) + E_U[u'(t + \tau)]\}\, d\alpha,$$

where only positive values of the integrand are considered, and

$$E_U[r_{Y|3}(t, \tau)] = \int_0^{\tau} \int_0^{\tau - \alpha} f_X(\tau - \alpha - \beta) f_X(\beta) f_U[\theta - h(\tau) - h(\alpha + \beta) - h(\alpha), t + \tau] \cdot \{h'(\tau) + h'(\alpha + \beta) + h'(\alpha) + E_U[u'(t + \tau)]\}\, d\beta\, d\alpha.$$

If $h(\tau) \to 0$ for large τ, then

$$E_U[r_{Y|1}(t, \tau)] \cong f_U[\theta, t + \tau] \cdot E_U[u'(t + \tau)],$$

$$E_U[r_{Y|2}(t, \tau)] \cong \int_0^\tau f_U[\theta - h(\alpha), t + \tau]\{h'(\alpha) + E_U[u'(t + \tau)]\} f_X(\tau - \alpha)\,d\alpha,$$

$$E_U[r_{Y|3}(t, \tau)] \cong \int_0^\tau f_U[\theta - h(\alpha), t + \tau]\{h'(\alpha) + E_U[u'(t + \tau)]\} \cdot \int_0^{\tau-\alpha} f_X(\tau - \alpha - \beta) f_X(\beta)\,d\beta\,d\alpha,$$

so that for $\tau \gg 0$

$$R_{XY}(t, \tau) \cong \lambda f_U(\theta, t + \tau) E_U[u'(t + \tau)] + \lambda \int_0^\tau R_{XX}(\tau - \alpha) f_U[\theta - h(\alpha), t + \tau] \cdot \{h'(\alpha) + E_U[u'(t + \tau)]\}\,d\alpha, \quad (11)$$

where $\lambda R_{XX}(\tau)$ is the autocorrelation function of $X(t)$. Note that if the process $U(t)$ is stationary then $E_U[u'(t + \tau)] = 0$ and the first term drops out.

In general, then, the cross-correlation function for short lags is related to the derivative $h'(t)$, while for large lags it is related to the autocorrelation function of the input process. The presence of the derivative is of some practical significance for two reasons: (*1*) PSP's with small amplitudes but large rates of rise will be readily detected in the cross-correlation function while they may be obscured by noise in intracellular recordings. (*2*) Analysis of the shape of the cross-correlation can provide information as to the location of the synapse on the neuron if the neuron is of the integrative type treated by Rall (1967). I will come back to this second point in a subsequent section.

NUMERICAL AND SIMULATION RESULTS

Approximate Solutions for the Leaky Integrator

Numerical solutions for $R_{XY}(t, \tau)$ require that approximations for $f_U(u, t)$ be used. If it is assumed that (*1*) the rate of the input process is small compared with the rate constant ϵ and (*2*) $h(t)$ is small then a reasonable approximation to $f_U(u, t)$ is $f_U(u)$ the membrane potential density function for stationary $U(t)$ and no threshold condition. Also, I take the input process $X(t)$ to be a Poisson process whose autocorrelation function $R_{XX}(\tau) = \lambda\delta(\tau) + \lambda^2$. This white noise process excites the system at all possible frequencies, so it is a "universal input." For linear systems cross-correlation of the output with a white noise input is appealing in that the cross-correlation function is proportional to the impulse response $g(t)$ of the system, i.e., $R_{XY}(\tau) = \lambda g(\tau)$. For nonlinear systems there is no such simple correspondence, a treatment such as that of Weiner (1958) involving higher order cross-correlation kernels being necessary for a more complete description (see also Marmarelis and Naka, 1973). Such a treatment, however, is beyond the scope of this paper.

With $X(t)$ a Poisson process $f_U(u)$, while not directly known, can be determined from its Fourier transform or characteristic function $\phi(j\omega)$ (Rice, 1944).

$$\phi(j\omega) = \int_{-\infty}^{\infty} f_U(u) e^{j\omega u} du = P(\omega) + jQ(\omega),$$

$$\phi(j\omega) = \exp\left\{\lambda \int_0^{\infty} (\exp[j\omega h(t)] - 1) dt\right\}, \tag{12}$$

where $j = \sqrt{-1}$. $f_U(u)$ may be obtained from the inverse cosine transform of the real part of $\phi(j\omega)$, $P(\omega)$, as

$$f_U(u) = \frac{2}{\pi} \int_0^{\infty} P(\omega) \cos \omega u d\omega. \tag{13}$$

When $h(t) = a \exp(-\epsilon t)$

$$P(\omega) = \cos[(\lambda/\epsilon) \operatorname{Si}(\omega a)] \exp\{(\lambda/\epsilon)[\operatorname{Ci}(\omega a) - \gamma - \ln \omega a]\}, \tag{14}$$

where γ is Euler's constant and $\operatorname{Si}(z)$ and $\operatorname{Ci}(z)$ are the sine and cosine integrals. Eq. 13 was evaluated numerically for three values of $a = 0.5$, 0.7, and 0.9; $\lambda = 50/s$; and $1/\epsilon = 8$ ms. ϵ was chosen so as to be compatible with the simulation program (see below) and is consistent with time constants reported for real neurons (Rall, 1957; Coombs et al., 1959). A further numerical integration gave the distribution function $F_U(u)$ from which the required probabilities, e.g., $P[\theta - a < U(t) \leq \theta]$, could be determined. A plot of the density function $f_U(u)$ is shown in Fig. 3 for these particular

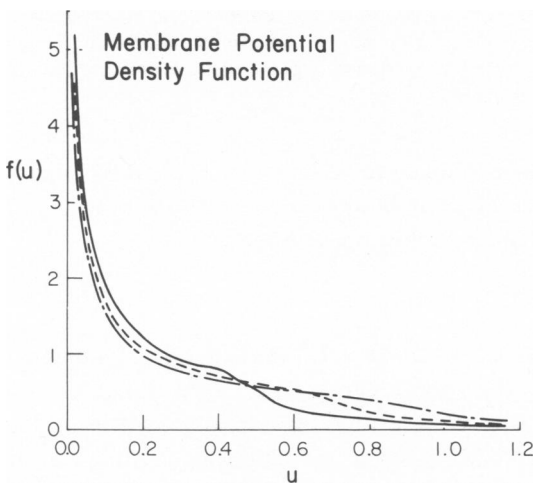

FIGURE 3 Steady-state membrane potential density functions $f_U(u)$ for the case $h(t) = a \exp(-\epsilon t)$, Poisson input with mean rate $\lambda = 50/s$, and $a = 0.5$ (_____), $a = 0.7$ (------) and $a = 0.9$ (—·—·—). The values were obtained by numerical inversion of the characteristic function of a shot process without the threshold condition (see text).

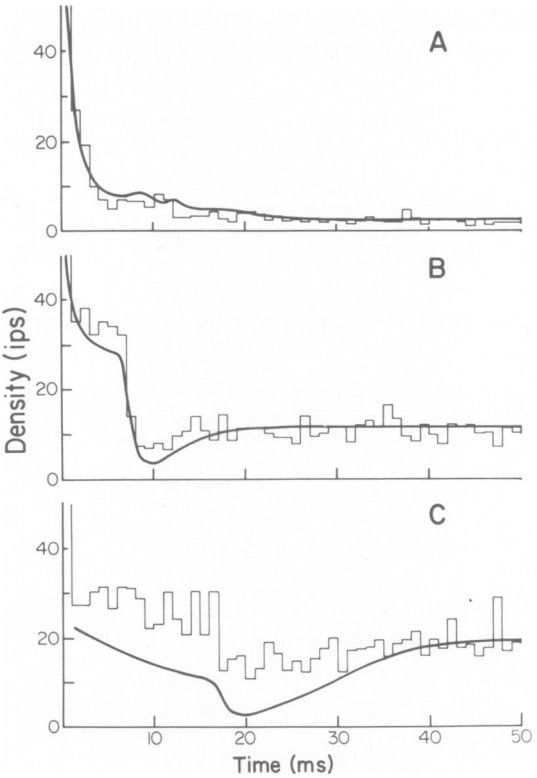

FIGURE 4 Cross-correlation functions of the model with a Poisson input of mean rate $\lambda = 50/s$. The impulse response $h(t) = a \exp(-\epsilon t)$ ($1/\epsilon = 8$ ms) and $a = 0.5$ (*A*), 0.7 (*B*), and 0.9 (*C*). The solid lines are from numerical solutions of text Eq. 9 while the histograms were obtained by simulation with NCMP. Note the minimum correlation even though only excitation is present (*B* and *C*). Not shown are the delta functions and large bin counts at time zero resulting from the derivative of the leading edge of $h(t)$.

variables. If threshold θ is taken to be one, without loss of generality, then it may be noted that one source of error in approximating $f_U(u, t)$ with $f_U(u)$ is the small but finite amount of probability falling above threshold.

RESULTS

With these values of a, λ and ϵ and $\theta = 1$, I evaluated Eq. 9 numerically and the results are shown in Fig. 4 by the smooth curves. Figs. 4 A, B, and C correspond to $a = 0.5$, 0.7, and 0.9. The unsmoothed histograms were obtained using the Neuronal Circuit Modeling Program (NCMP) (Knox and Poppele, 1973). One model neuron with $h(t) = a \exp(-\epsilon t)$, (compartment 0), where $1/\epsilon = 8$ ms, was stimulated with a Poisson input at $\lambda = 50/s$. The estimate of the cross-correlation function was generated by NCMP by binning counts for all outputs following any given input. The ordinates of Fig. 4 are in terms of the density $r_{Y|X}(\tau)$ with units of impulses per second. For

a = 0.5 and 0.7 the agreement between Eq. 9 and the simulation is good (Fig. 4 A and B). At a = 0.9, however, the approximation for $f_U(u, t)$ is no longer adequate (Fig. 4 C) although qualitatively the two results are similar. The limiting factor is likely to be the nonstationarity of $U(t)$ rather than the boundary condition of the threshold. At τ = 0 the cross-correlation function displayed an impulse as predicted, the large bin counts not being shown so as to preserve detail. For large τ the function assumes a constant value proportional to the input rate. For short lags the cross-correlation function is quite complicated, looking nothing like the underlying PSP, and when a = 0.7 (Fig. 4 B) actually indicates a minimum correlation at approximately τ = 10 ms. This minimum is still somewhat evident when a = 0.9 (Fig. 4 C) at τ = 20 ms. A series of simulations in which λ ranged from 40 to 100/s showed that the minimum is a consistent feature of the cross-correlation when the parameter a is greater than 0.5 of threshold and $h(t) = a \exp(-\epsilon t)$. NCMP allows simulation of two additional PSP shapes of the form $t \exp(-\epsilon t)$ and $t^2 \exp(-\epsilon t)$, (compartments 1 and 2), mimicking inputs located one and two space constants from the site of spike production in a single unbranched equivalent cable. When these PSP shapes were used in a similar series of simulations no minimum correlation was observed. This phenomenon of a minimum correlation where there is only excitation is therefore associated with synaptic input close to the spike initiation region of the cell of an amplitude larger than approximately half threshold.

In Fig. 5 are plotted comparable simulation results for compartment 1 (Fig. 5 A and B) and 2 (C and D). The mean rate of the Poisson input was λ = 50/s, and peak PSP amplitudes were 0.5 (A and C) and 0.7 (B and D). In these cases there are no delta functions at the origin; rather, the primary synaptic effect extends to lags τ that are approximately the times during which the PSP is rising. This behavior is explain-

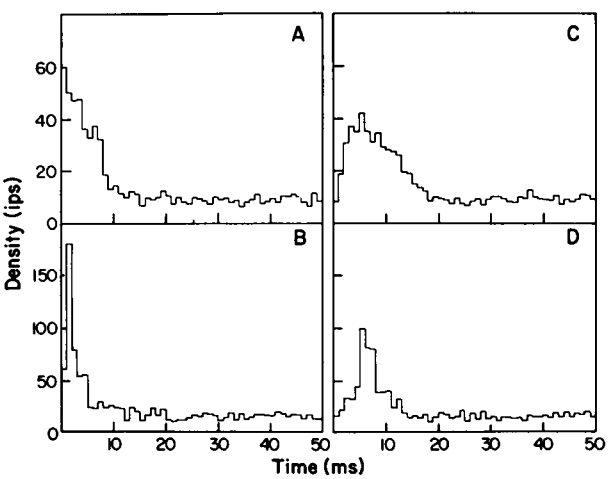

FIGURE 5 Cross-correlation histograms obtained by simulation. Poisson process input with λ = 50/s, and $h(t)$ of the forms $t \exp(-\epsilon t)$ (*A* and *B*) and $t^2 \exp(-\epsilon t)$ (*C* and *D*). Peak PSP amplitudes were 0.5 (*A* and *C*) and 0.7 (*B* and *D*).

able on the basis of results of the preceding section, namely that the term $E_U[r_{Y|1}(t, \tau)]$ should dominate near $\tau = 0$, and that, from Eq. 11, $R_{XY}(t, \tau)$ assumes a constant value for large τ and a Poisson input. Given the low mean output rates in these cases (10–15 ips), $U(t)$ can be expected to be nearly stationary and $E_U[u'(t + \tau)] \cong 0$ so that $E_U[r_{Y|1}(t, \tau)] \cong f_U[\theta - h(\tau), t + \tau]h'(\tau)$ for $h'(\tau) \geq 0$. The contributions of the next few terms of the series of Eq. 10 will, however, make the duration of the initial peak of $R_{XY}(t, \tau)$ deviate from the time over which $h'(\tau) \geq 0$.

The Cross-Correlation Function as an Estimator of PSP Shape

As has been seen the cross-correlation function contains information on the derivative of the PSP. The question naturally arises as to what information this fact provides on possible location of a synapse on a cell and the cell's apparent time constant. As Rall (1967) has pointed out shape analysis of the PSP cannot uniquely answer this question since slowly rising and falling PSP's can be due to combinations of inputs along a dendrite as well as to single inputs located some distance from the soma. Such shape analysis is useful, however, and becomes more reliable the closer the synapse is to the soma of a cell. For inputs located on the soma the PSP at the spike initiation region rises abruptly to its peak and an impulse will appear in the cross-correlation at $\tau = 0$. Unfortunately, in this case, no information is contained in this impulse as to membrane time constant.

For inputs located away from the soma a shape analysis of the cross-correlation function becomes somewhat more productive, as is suggestive of the examples of Fig. 5. However, from the general form of $R_{XY}(t, \tau)$ we can expect such an analysis to yield biased estimates of the PSP shape, due to the unknown weighting contributed by $f_U(u, t)$, and the amount of bias can only be determined empirically. It is possible also that with different choices of input, one input process will lead to better estimates of PSP shape than another. In particular, I shall consider $X(t)$ to be periodic in one case and Poisson in another.

Inspection of Eq. 11 shows that if $X(t)$ is taken to be the periodic pulse train $\sum_n \delta(t - nT)$ with time between pulses T then $R_{XX}(\tau) = \lambda \sum_n \delta(\tau - nT)$ and for $\tau \gg 0$

$$R_{XY}(t, \tau) = \lambda^2 \sum_n f_U[\theta - h(\tau - nT), t + \tau]\{h'(\tau - nT) + E_U[u'(t + \tau)]\},$$

that is, the sum of shifted functionals of the form $f_U[\theta - h(\tau), t + \tau]\ \{h'(\tau) + E_U[u'(t + \tau)]\}$ which I shall call the *primary correlation kernel.* Note that by integrating this kernel one obtains a distorted estimate of the shape of the initial portion of the PSP. One caveat is in order. If the only source of excitation of the cell is a periodic (i.e. nonrandom) pulse train then $U(t)$ is a deterministic function and $f_U(u, t)$ is degenerate. The primary correlation kernel then degenerates to an impulse whose strength is related to $h'(\tau)$. In order that the primary correlation kernel be continuous, so that some estimate of its shape can be made, $f_U(u, t)$ must be continuous at the

time of threshold crossing. If the cell receives excitatory input uncorrelated with this special $X(t)$ or is inherently spontaneous then this condition is fulfilled. Note that this situation in part determines $f_U(u, t)$ and that the cross-correlation function will also evidence secondary effects in addition to primary effects treated in previous sections. The requirement of some exogenous noise will then alter somewhat the form of the primary correlation kernel. To what extent can only be determined by means of simulation techniques. Before presenting such simulation results for the periodic input train two general observations can be made on the distortions in the shape of the PSP one would obtain by integrating the primary correlation kernal: (*1*) With exogenous noise or pacemaker activity $E_U[u'(t + \tau)]$ will in general be positive, i.e. there is a drift towards threshold. Hence, the quantity $h'(\tau) + E_U[u'(t + \tau)]$ will remain positive past the time to peak, t_p, of the PSP, and the width of the kernel, $\hat{t}_p$, or the *primary correlation time,* will in general overestimate t_p. The higher the spontaneous firing rate of the cell the larger $\hat{t}_p$ will be in comparison to t_p. (*2*) $f_U(u, t)$ will in general decrease with increasing u near threshold, and the functional $f_U[\theta - h(\tau), t + \tau]$ will increase with τ if $h(\tau)$ increases with τ. The primary correlation kernel will thus rise faster than $h'(\tau)$ and, hence, integrating the kernel will give a function which rises faster than the PSP. The faster the cell is firing the more time $U(t)$ spends near threshold and $f_U(u, t)$ will decrease even more sharply there, leading to an even greater rate of rise of the kernel compared to the PSP. In general, then, analysis of the primary correlation kernel leads to an overestimation of both the time to peak and the rise time of the PSP.

As an example of a shape analysis based on the primary correlation kernel, NCMP was used to generate cross-correlation functions for the case of a model neuron with periodic stimulation at 20/s, spontaneous rate (in the absence of stimulation) of 10/s and internal Gaussian noise with standard deviation of 0.2 times threshold. Fig. 6 depicts a representative cross-correlation function in the case when compartment 2 was stimulated, the peak PSP amplitude being 0.6 of threshold. The primary correlation time, $\hat{t}_p$, was estimated by eye to be 15 ms compared with an actual time to peak of the PSP of 16 ms. In the inset of Fig. 6 the numerically integrated histogram of the kernel along with a least squares fit of the function $t^p \exp(-pt/\hat{t}_p)$ are shown.

This function is obtained by making use of the relation $\epsilon = p/t_p$. In this case $p = 1.71$ after normalizing the maximum value of the function to the maximum histogram value. The ordinate values in the inset are arbitrary. Fig. 7 summarizes the results of a number of simulations in which the parameters were as given above but with varying peak amplitude of the PSP. Results for compartments 1 and 2 are given by filled and open circles. The primary correlation time, $\hat{t}_p$, (Fig. 7 A) is seen to be in general greater than the time to peak of the PSP (as indicated by the dashed lines for the two compartments) but is actually not too different for large amplitude PSPs. As may be seen in Fig. 7 B the least squares estimate of the parameter p is in general less than that for the PSP indicating that the integrated kernel rises faster than the PSP. In this example an estimate of the time constant $1/\epsilon$ could be had from the ratio $\hat{t}_p/p$.

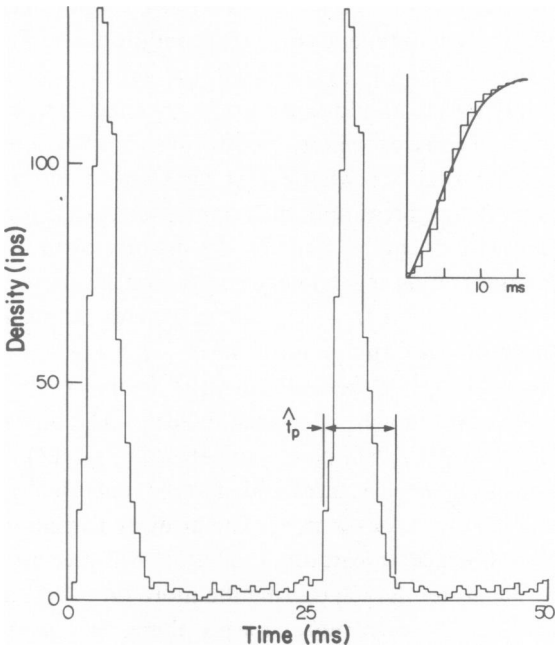

FIGURE 6 Cross-correlation using a periodic input pulse train. $h(t)$ of the form $t^2 \exp(-\epsilon t)$ and peak amplitude 0.6 of threshold. The width of the primary correlation kernel t_p is a biased estimate of the time to peak of $h(t)$. Numerically integrating the kernel (inset) gives an approximate shape for the leading edge of $h(t)$. In general the profile so obtained has a faster rate of rise than the actual $h(t)$.

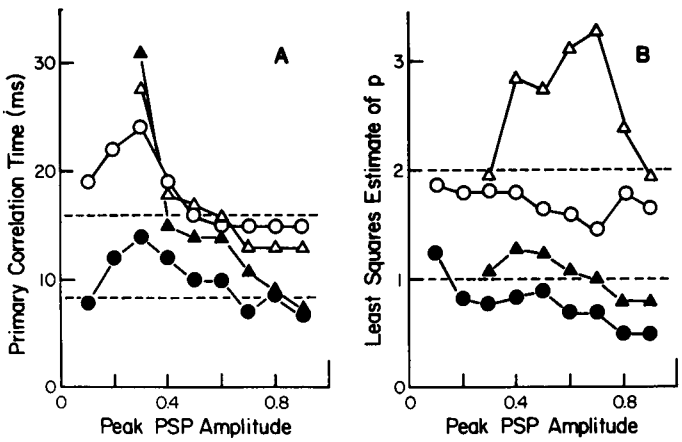

FIGURE 7 (*A*) The primary correlation time, $\hat{t}_p$, as obtained from simulations by cross-correlating with a periodic input (circles) and Poisson input (triangles) for $h(t)$ of the forms $t \exp(-\epsilon t)$ (filled symbols) and $t^2 \exp(-\epsilon t)$ (open symbols) as a function of peak amplitude of $h(t)$ when threshold $\theta = 1$. $\hat{t}_p$ in general tends to overestimate the actual time to peak of $h(t)$ (as shown by the dashed lines) particularly for small peak amplitudes and Poisson input. (*B*) Estimates of the shape of $h(t)$ obtained by fitting the function $t^p \exp(-pt/\hat{t}_p)$ to integrated kernels such as the one of the inset of Fig. 6. p in general underestimates the order of $h(t)$ when periodic inputs are used and overestimates it when using Poisson inputs. Open symbols apply to the case $h(t) \sim t^2 \exp(-\epsilon t)$ and filled symbols to $t \exp(-\epsilon t)$.

Note that since $\hat{t}_p$ overestimates t_p and p is an underestimate of the actual compartment this ratio significantly overestimates the time constant.

As discussed above, with a Poisson input $R_{XY}(t,\tau)$ will be given approximately by the primary correlation kernel near $\tau = 0$, although it will be influenced by the next terms of the series Eq. 10. Numerical integration of the initial peak in $R_{XY}(t,\tau)$ with Poisson inputs, such as those in Fig. 5, will again yield biased estimates of t_p and p. The results of such computations for compartments 1 and 2 are shown in Fig. 7 by filled and open triangles. Peak PSP amplitude was varied while the mean input rate was held constant at $\lambda = 50/s$. Data are not shown for PSP amplitude of 0.1 and 0.2 since output rates become practically zero in these cases. It can be concluded, at least for the conditions used, that the periodic input leads to better, albeit biased, estimates of PSP shape than does the Poisson input.

Even though the model considered is a simple one inclusion of additional desirable features such as refractoriness will not significantly affect the cross-correlation function under certain conditions. The structure of the cross-correlation function is determined first of all by events which place the membrane potential near threshold and secondly by the autocorrelation function of the input process. Under conditions of low output rates when intervals between output spikes remain substantially greater than any refractory period the history of events immediately following an output spike is all but lost when the membrane potential next crosses threshold. This will also apply to the case of any feedback inhibition, such as mediated by a recurrent interneuron, so long as the duration of feedback is short with respect to the output interspike interval. These qualitative observations suggest that when cross-correlation techniques are used to assess properties of neuronal networks such processes can go undetected using these techniques alone. The results also point out the desirability of using a periodic input in addition to the white noise Poisson process. In fact, the two may be used in combination as a stimulus to excite a normally quiescent cell. Cross-correlation of the output with the periodic stimulus would then give the primary correlation kernel from which estimates of the parameters of the PSP could be made. These considerations do not detract from the use of a Poisson input in the analysis of neuronal systems. Such an input avoids phase-locking, or entrainment, of the system. The Poisson process contains all frequencies equally weighted with random phases. Intuitively, the response to this input should therefore completely characterize certain types of nonlinear systems. As Wiener (1958) has shown (see also, Lee and Schetzen, 1961), Gaussian white noise completely defines any time-invariant nonlinear system with finite memory. A corresponding formalism for Poisson point processes has not been developed, so far as I know, and remains a topic for further research.

This work was supported by U. S. Public Health Service Grant NS02567 and by a grant from the University of Minnesota Graduate School. IBM 1800 computer facilities were made available by a grant from the U. S. Air Force Office of Scientific Research, AFSC-1221.

Received for publication 9 November 1973 and in revised form 12 April 1974.

REFERENCES

BARTLETT, M. S. 1963. *J. R. Stat. Soc. B.* **25**:264.

BRYANT, H. L., A. R. MARCOS, and J. P. SEGUNDO. 1973. *J. Neurophysiol.* **36**:205.

COOMBS, J. S., D. R. CURTIS, and J. C. ECCLES. 1959. *J. Physiol. (Lond.).* **145**:505.

FETZ, E. E., and G. L. GERSTEIN. 1963. *Quarterly Progress Report M.I.T. Research Laboratory of Electronics.* **71**:249.

JOHANNESMA, P. I. M. 1968. *In* Neural Networks. E. R. Caianiello, editor. Springer-Verlag, Berlin. 116.

KNIGHT, B. W. 1972. *J. Gen. Physiol.* **59**:734.

KNOX, C. K., and R. E. POPPELE. 1973. *Comput. Biomed. Res.* **6**:487.

LEE, Y. W., and M. SCHETZEN. 1961. *Quarterly Progress Report M.I.T. Research Laboratory of Electronics.* **60**:118.

MARMARELIS, P. Z., and K. NAKA. 1973. *J. Neurophysiol.* **36**:605.

MOORE, G. P., J. P. SEGUNDO, D. H. PERKEL, and H. LEVITAN. 1970. *Biophys. J.* **10**:876.

PARZEN, E. 1962. Stochastic Processes. Holden-Day, Inc., San Francisco, Calif. 146.

RALL, W. 1957. *Science (Wash. D.C.).* **126**:454.

RALL, W. 1967. *J. Neurophysiol.* **30**:1138.

RICE, S. O. 1944. *Bell Syst. Tech. J.* **23**:282.

STEIN, R. B. 1965. *Biophys. J.* **5**:173.

STEIN, R. B., A. S. FRENCH, and A. V. HOLDEN. 1972. *Biophys. J.* **12**:295.

WIENER, N. 1958. Nonlinear Problems in Random Theory. John Wiley & Sons, Inc., New York.